



Supplement of

Characteristics of surface physical and biogeochemical parameters within mesoscale eddies in the Southern Ocean

Qian Liu et al.

Correspondence to: Yingjie Liu (yjliu@qdio.ac.cn)

The copyright of individual parts of the supplement might differ from the article licence.

Text S1. Method to calculate eddy-centric composite maps

We extract data from $-2R$ to $2R$ to include the interactions between eddies and the surrounding waters and interpolate them onto an evenly spaced 17 by 17 grid to create the surface composite patterns. For daily SST and Chl-*a*, we perform the eddy-centric composite method matching eddies and variables on the same day and calculate the mean value. In contrast, for 5 monthly DIC and $p\text{CO}_2$, we calculate the eddy-centric composite maps using all eddies of the same month, along with DIC and $p\text{CO}_2$ data from that month, and obtain the mean value.

Text S2. Method to obtain the gradients of SST, Chl-*a*, and DIC

The gradients of interior points are computed using a first-order central difference in Eq. (1) (Quarteroni et al., 2006). The gradients for boundaries are computed using forward/backward differences in Eq. (2)/Eq. (3). The average gradient is computed using the formula in Eq. (4).

$$grad(\mu_x) = \frac{\mu_{x+1} - \mu_{x-1}}{2} \quad (1)$$

$$grad(\mu_y) = \frac{\mu_{y+1} - \mu_{y-1}}{2} \quad (1)$$

$$grad(\mu_x) = \mu_{x+1} - \mu_x \quad (2)$$

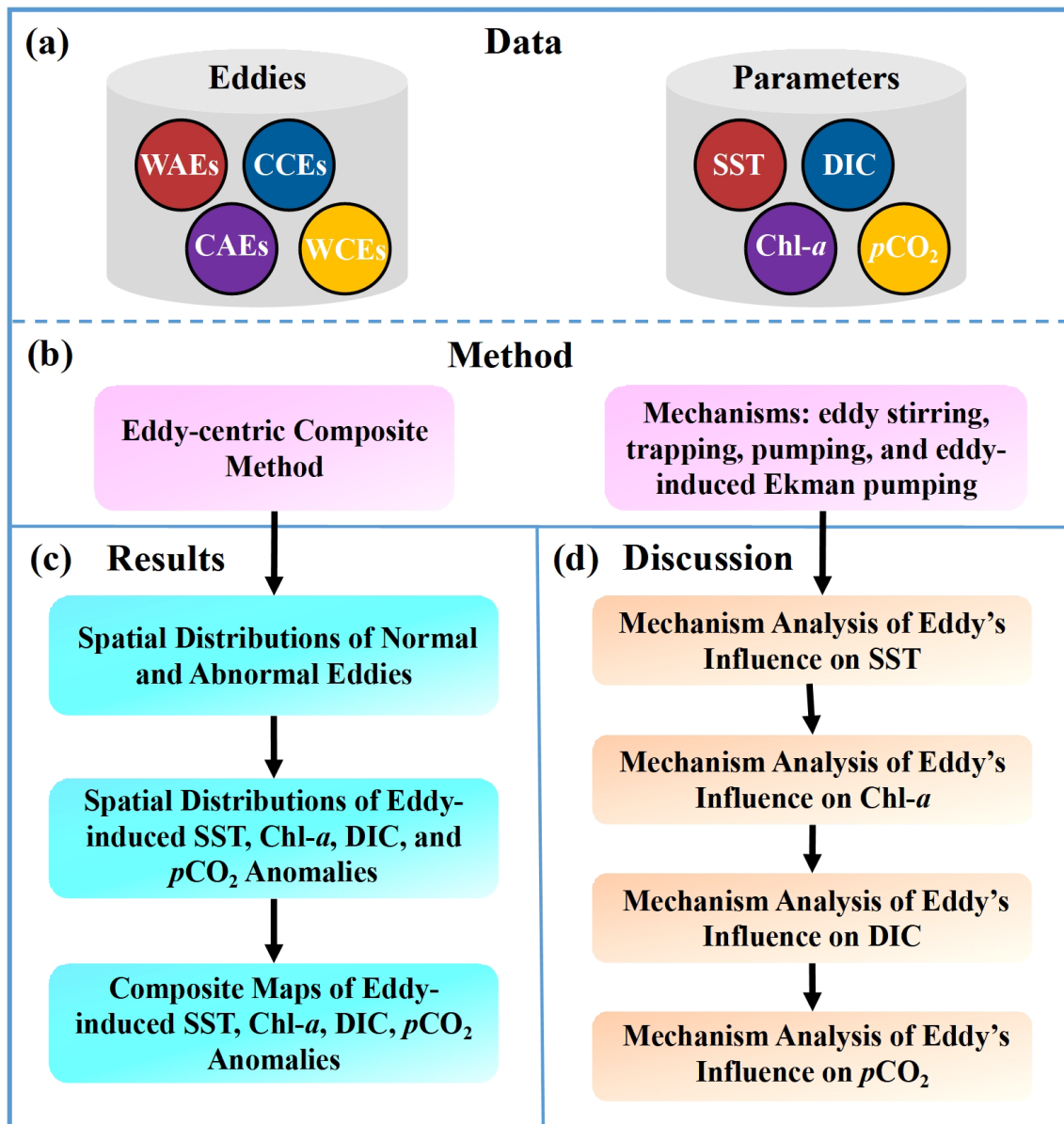
$$grad(\mu_y) = \mu_{y+1} - \mu_y \quad (2)$$

$$grad(\mu_x) = \mu_x - \mu_{x-1} \quad (3)$$

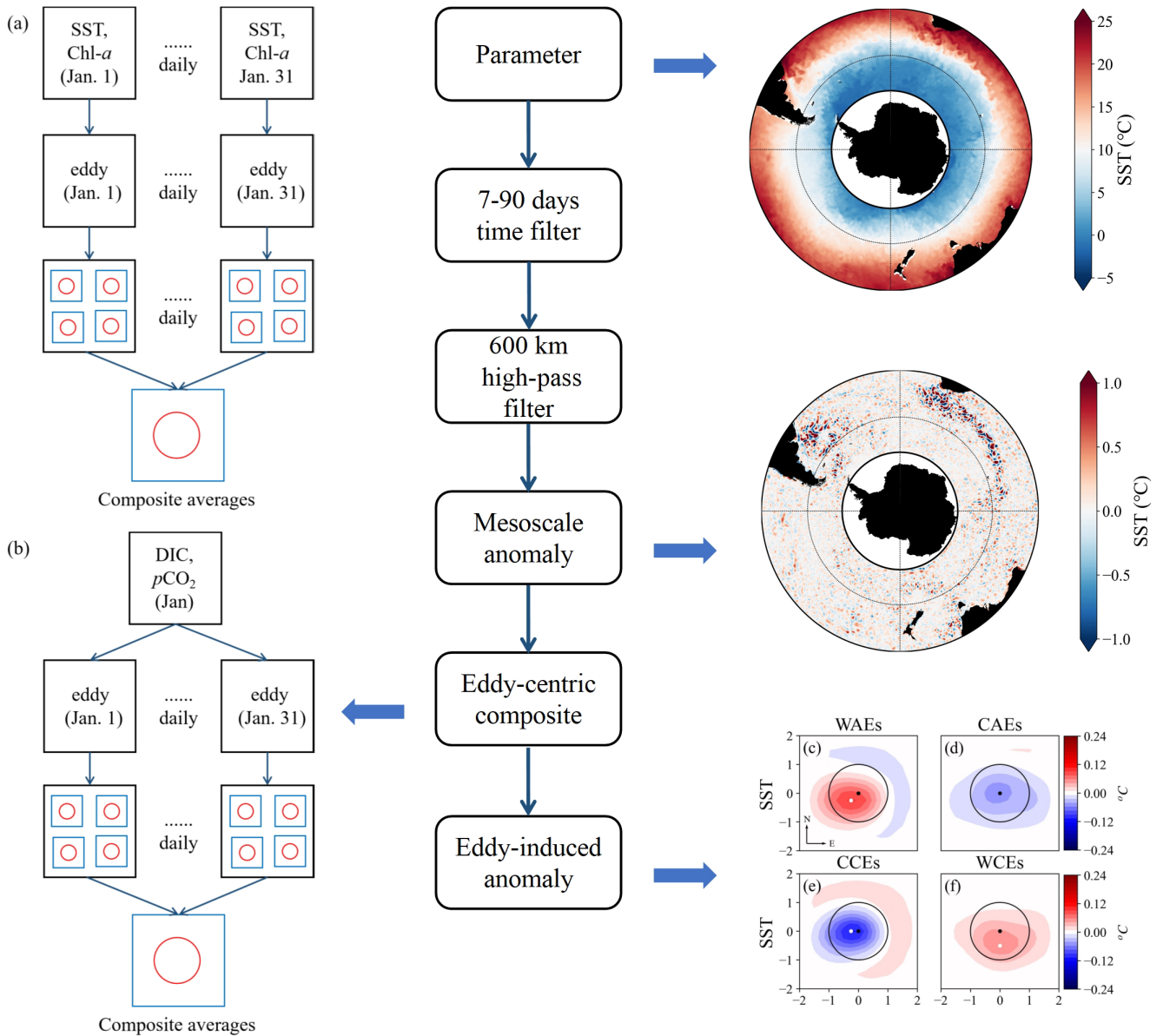
$$grad(\mu_y) = \mu_y - \mu_{y-1} \quad (3)$$

$$\overline{grad} = \frac{\sum_0^{n-1} \left(\sqrt{grad_i(\mu_x)^2 + grad_i(\mu_y)^2} \right)}{n} \quad (4)$$

15 where μ denotes climatological averages of normalized SST, Chl-*a*, and DIC in the SO during the period 1996–2015. $grad(\mu_x)$ and $grad(\mu_y)$ represent the gradients in the meridional and zonal directions. n represents the total number of data points. \overline{grad} is the final average gradient.

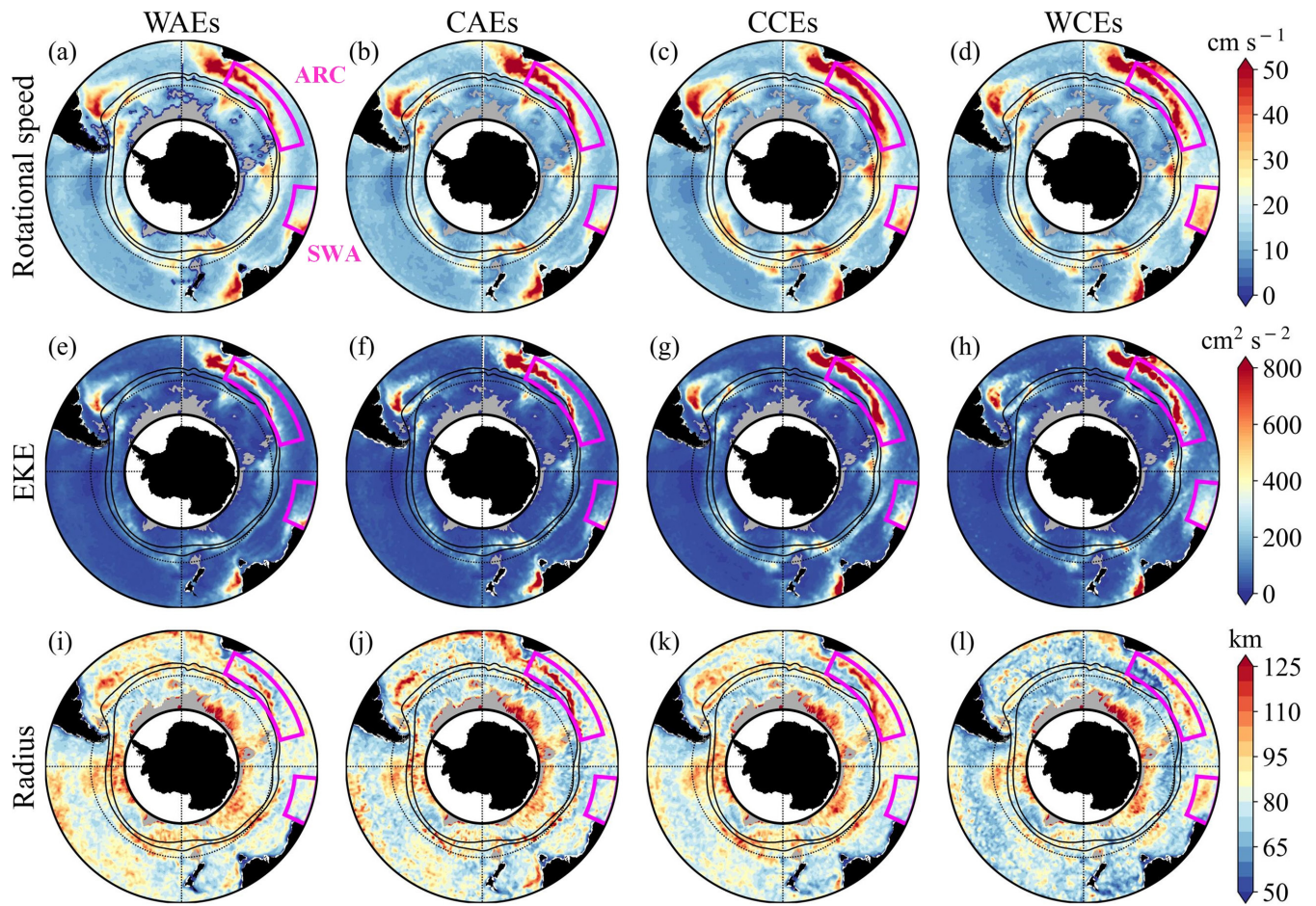


20 **Figure S1.** Research structure. Based on the eddy dataset, satellite SST and Chl-*a*, as well as observation-based reconstruction of DIC and *p*CO₂ from 1996 to 2015 in the SO, we use the eddy-centric composite method to conduct the composite patterns of SST, Chl-*a*, DIC, and *p*CO₂ associated with eddies. And then, we use mechanisms, including eddy stirring, trapping, pumping, and eddy-induced Ekman pumping, to analyze the modulation of eddies to SST, Chl-*a*, DIC, and *p*CO₂.



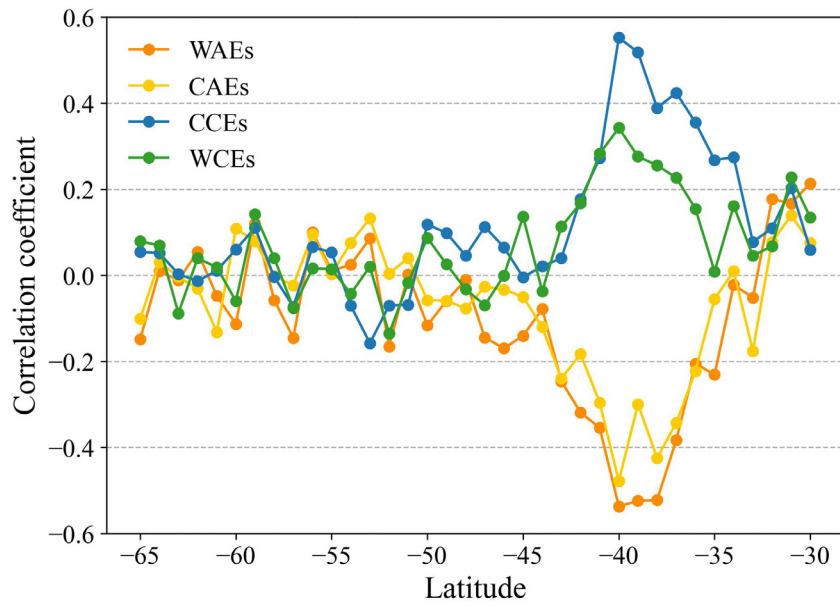
25

Figure S2. Schematic of eddy-induced anomaly composite method. The left column depicts the schematic of the eddy-centric composite method for daily (a) SST and Chl-*a* and monthly (b) DIC and $p\text{CO}_2$, taking January as an example. The middle column illustrates the method structure. The right column showcases the resulting output of the corresponding processing, taking SST as an example.



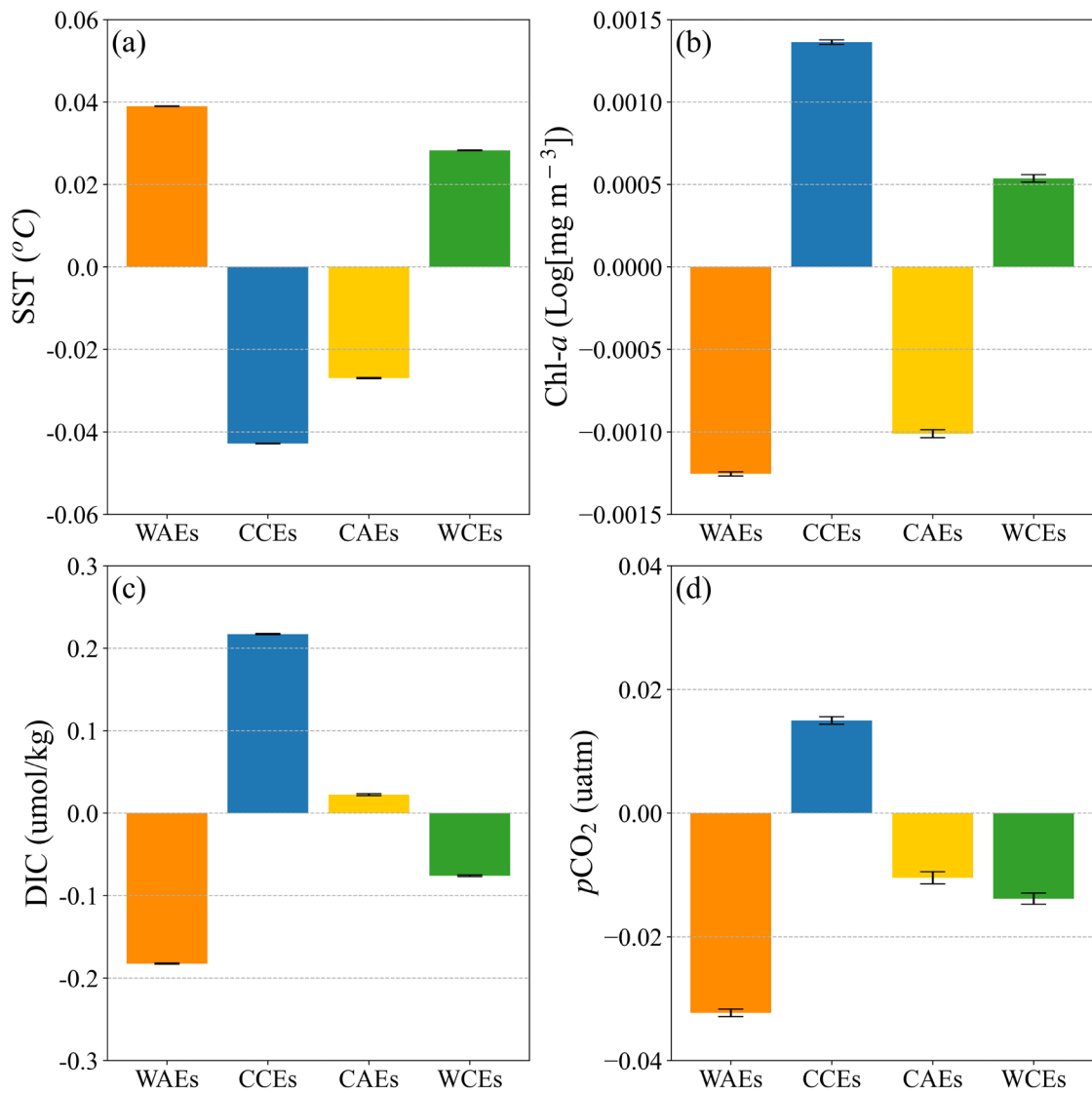
30

Figure S3. Spatial distribution of eddy properties, including (a–d) rotational speed, (e–h) EKE, and (i–l) radius in the Southern Ocean from 1996 to 2015. From left to right, columns represent four kinds of eddies. Black solid lines show the mean northern (SAF) and southern (PF) positions of the ACC major fronts (Sallée et al., 2008). The black dotted circle is 50° S. The magenta boxes represent ARC and SWA regions.



35

Figure S4. Correlation coefficients between Chl-*a* anomalies and eddy amplitudes along latitudes. The correlation coefficients range from -1 to 1 , where -1 and 1 indicate perfect negative and positive linear correlations, respectively, and 0 signifies no linear correlation. Solid lines in different colors denote four kinds of eddies.



40 **Figure S5.** Averages (bars) and standard error (error bars) of SST, Chl-*a*, DIC, and $p\text{CO}_2$ anomalies within WAEs, CCEs, CAEs, and WCEs.

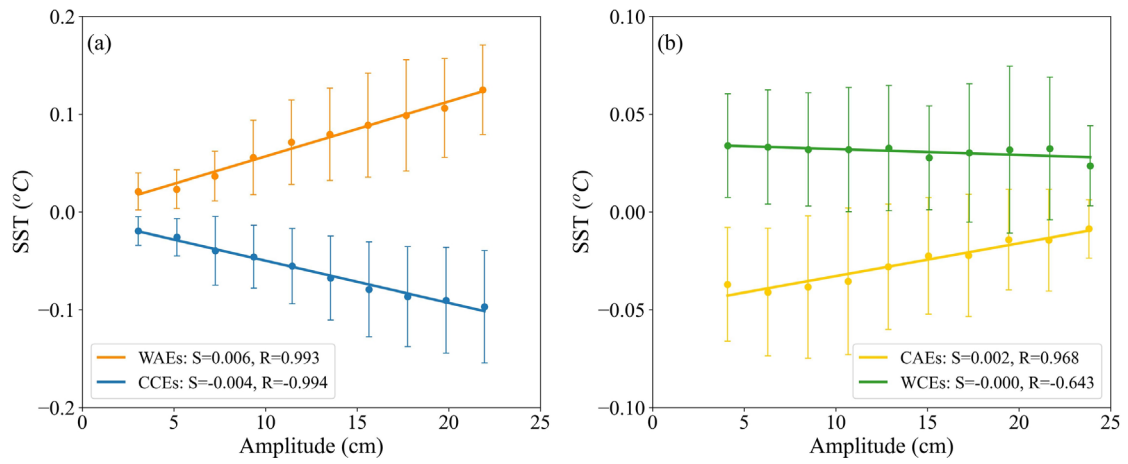


Figure S6. The mean SST anomaly within (a) “normal” eddies and (b) “abnormal” eddies as a function of eddy amplitude in the SO. Dots denote the values averaged at the binned amplitude intervals of 2 cm. Solid lines denote the regression lines obtained from least squares fitting with S being the slope and R the correlation coefficient. Solid lines in different colors denote four kinds of eddies.

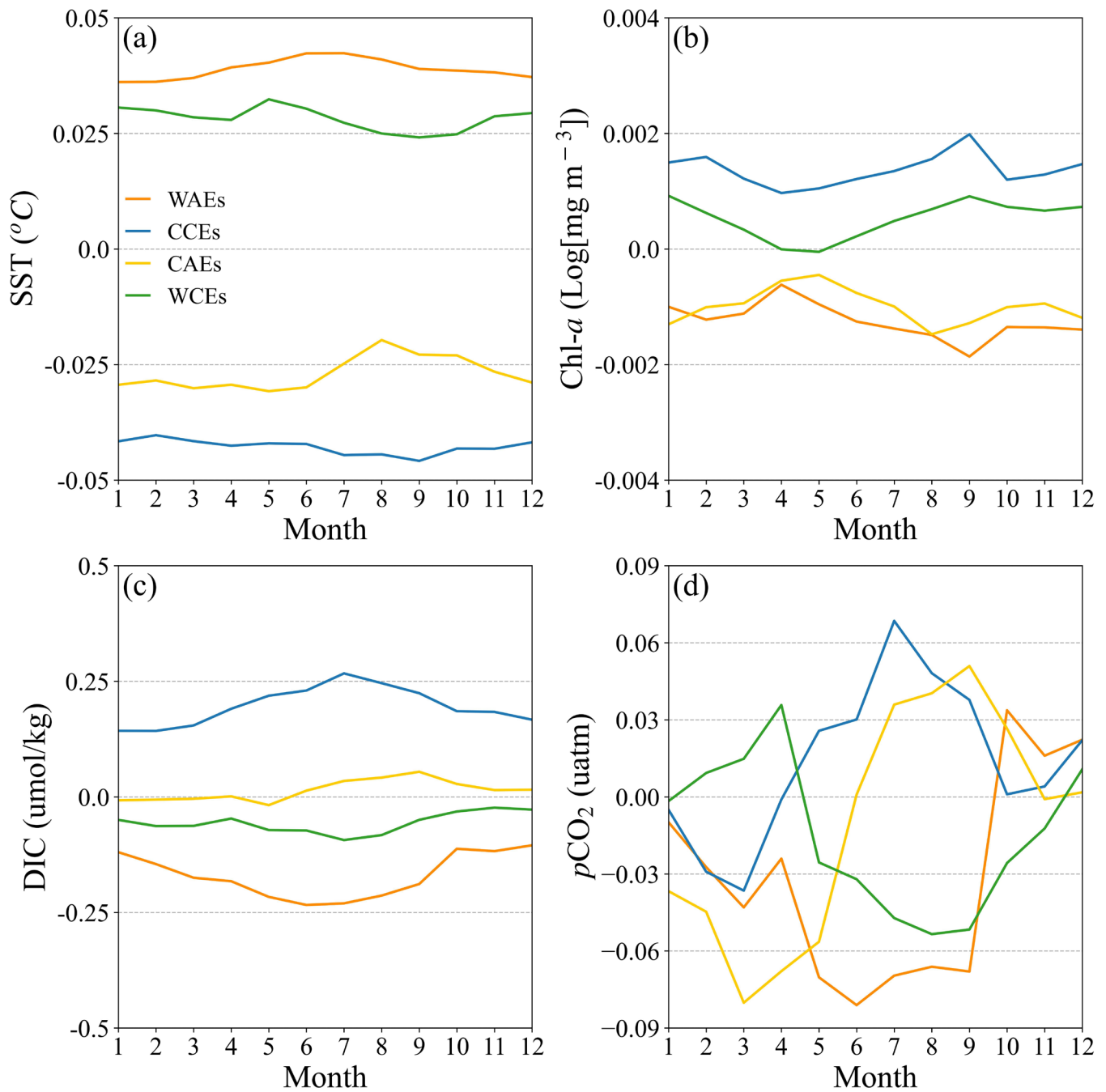


Figure S7. Variations in monthly mean eddy-induced anomalies, including (a) SST, (b) Chl- a , (c) DIC, and (d) $p\text{CO}_2$ in the SO from 1996 to 2015. Solid lines in different colors denote four kinds of eddies.

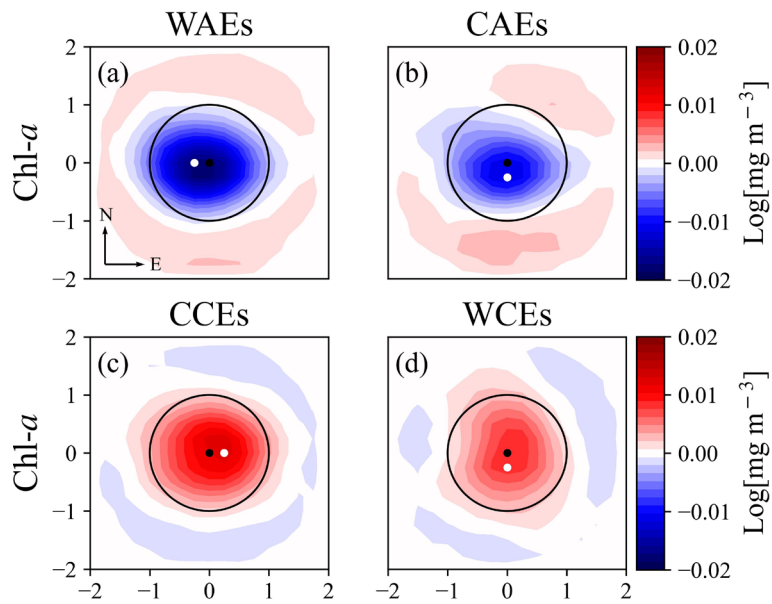


Figure S8. Eddy-centric composite averages for Chl-*a* anomalies in the BMC. On each map, a black dot denotes the eddy center, and a white dot denotes the center location of variables (defined by the location of the extremum value). Contour intervals are every 0.0013 Log[mg m⁻³] for Chl-*a*.

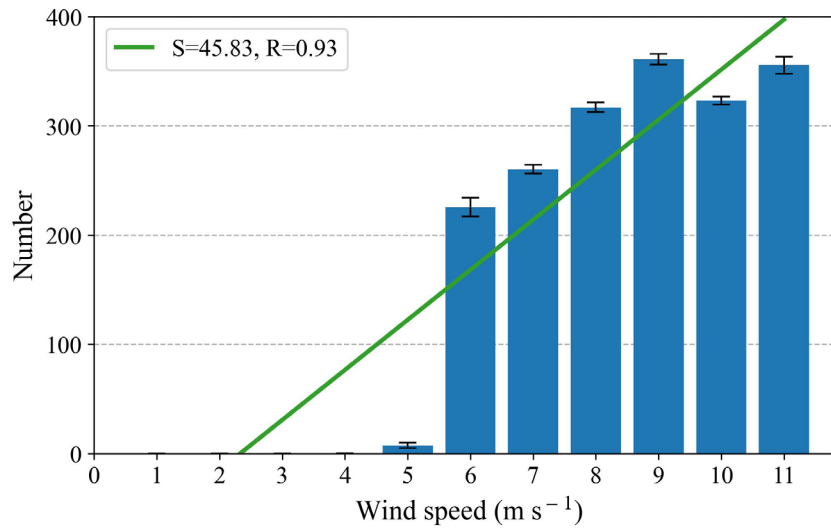


Figure S9. The mean number of “abnormal” eddies as a function of wind speed in the SO. The blue bars denote the number of “abnormal” eddies occurrence in each $1^\circ \times 1^\circ$ latitude-longitude bin over the analyzed period 1996–2015, which is averaged at the binned wind speed intervals of 1 m s^{-1} . The black error bars denote the standard error. The green line denotes the regression line obtained from least squares fitting with S being the slope and R the correlation coefficient.

Table S1. Spatial and temporal resolutions and filtering methods of SST, Chl-*a*, DIC, and *p*CO₂.

	Temporal resolution	Spatial resolution	Temporal filter	Spatial filter
SST	daily	0.25° × 0.25°	7-90 days band-pass filter	
Chl- <i>a</i>	daily	4 km × 4 km		spatial high-pass filtering with 6° × 6°
DIC	monthly	1° × 1°	subtracting the climatological averages	
<i>p</i> CO ₂	monthly	1° × 1°		

Table S2. The climatological characteristics of mesoscale eddies in the Southern Ocean from 1996 to 2015.

	WAEs/CAEs	CCEs/WCEs	“Normal”/“Abnormal”	AEs/CEs
Number	5,450,860/1,786,338	5,261,780/2,043,428	10,712,640/3,829,766	7,237,198/7,305,208
Amplitude (cm)	6.45/6.37	6.98/6.45	6.72/6.41	6.43/6.95
Rotational speed (cm s ⁻¹)	15.76/15.37	16.64/16.13	16.20/15.75	15.63/16.62
EKE (cm ² s ⁻²)	83.78/85.90	105.88/102.86	94.83/94.38	83.95/106.29
Radius (km)	88.62/87.24	87.54/82.96	88.08/85.10	88.82/87.21

65 **Table S3.** Number of AEs and CEs moving westward/eastward and northward/southward, including the overall eddies and eddies with lifetimes longer than 1 year.

	Eastward	Westward	Northward	Southward
AEs	7,924,626	9,261,954	9,266,102	7,920,478
CEs	8,387,806	9,300,955	9,824,357	7,864,404
AEs (>1 year)	44,184	323,242	294,536	72,890
CEs (>1 year)	97,955	294,167	140,362	251,760

Table S4. Averages and standard error (in parentheses) of SST, Chl-*a*, DIC, and *p*CO₂ anomalies within WAEs, CAEs, CCEs, and WCEs.

	WAEs	CAEs	CCEs	WCEs
SST	0.03898 (0.00007)	-0.02697 (0.00011)	-0.04284 (0.00007)	0.02828 (0.00010)
Chl- <i>a</i>	-0.00125 (0.00001)	-0.00101 (0.00002)	0.00136 (0.00001)	0.00054 (0.00002)
DIC	-0.18258 (0.00062)	0.02228 (0.00120)	0.21712 (0.00066)	-0.07598 (0.00106)
<i>p</i> CO ₂	-0.0323 (0.00061)	-0.01046 (0.00098)	0.01498 (0.00060)	-0.01383 (0.00090)

Table S5. Contributions of eddies to $p\text{CO}_2$ in different regions and seasons from 1996 to 2015. The contributions are the percentages of the eddy-induced $p\text{CO}_2$ anomalies maximum to the intra-annual variation of the corresponding variables.

Region	Eddy Type	Annual (%)	Winter (%)	Summer (%)
SO	WAEs	-0.87	-2.64	0.75
	CAEs	-0.27	1.04	-0.97
	CCEs	0.91	2.50	-0.67
	WCEs	-0.39	-1.40	0.80
SWA	WAEs	1.40	-1.76	4.12
	CAEs	-1.55	1.53	-2.06
	CCEs	-0.88	0.61	-1.91
	WCEs	1.49	-3.99	5.15
ARC	WAEs	-2.49	-3.15	-3.12
	CAEs	1.03	2.52	-1.40
	CCEs	2.53	5.03	2.06
	WCEs	-0.89	-1.19	1.26

Reference

- 75 Quarteroni, A., Sacco, R., and Saleri, F.: Numerical Mathematics (Texts in Applied Mathematics), Springer-Verlag, 2006.
- Sallée, J. B., Speer, K., and Morrow, R.: Response of the Antarctic Circumpolar Current to Atmospheric Variability, *J. Clim.*, 21, 3020-3039, <https://doi.org/10.1175/2007JCLI1702.1>, 2008.